Materials Letters 175 (2016) 63–67

Contents lists available at ScienceDirect

Materials Letters

journal homepage: www.elsevier.com/locate/matlet

Low pressure cold spray coating of Ti-6Al-4V with SiC-based cermet

D.I. Adebiyi [a,*], A.P.I. Popoola [a,*], I. Botef [b]

[a] Department of Chemical, Metallurgical and Materials Engineering, Tshwane University of Technology, P.M.B. X680, Pretoria 0001, South Africa
[b] School of Mechanical, Industrial and Aeronautical Engineering, University of the Witwatersrand, South Africa

ARTICLE INFO

Article history:
Received 14 September 2015
Received in revised form
23 March 2016
Accepted 28 March 2016
Available online 29 March 2016

Keywords:
Cold spray
Phase transformation
Peak shift
SiC
Porosity

ABSTRACT

The possibility of using the low pressure cold spray system to deposit SiC-based cermet on Ti-6Al-4V was investigated at 0.99 Mpa for 450, 500 and 550 °C. The characterizations of the coatings reveal that the initial phases in the feedstock powder were retained in the coatings. No detrimental phase transformation, decomposition and/or decarburization of the SiC. There was peak shift between the phases of the feedstock powder and that of the coatings. This is traced to impact-induced micro-straining, amorphization and grain refinement. Low pressure cold spray coating of Ti-6Al-4V with SiC-based cermet is plausible with partially homogenous distribution of the SiC, minimal porosity and improved microhardness value (approx 652 ± 12.7 $HV_{0.3}$) in the coating.

1. Introduction

Poor surface hardness has been one of the setbacks for the application of titanium alloy despite its excellent bulk properties [1]. This has necessitated various research works, including coating with different metallic and ceramic materials. The coating approach is essentially meant to improve the surface properties and performance without significantly altering the bulk chemistry and properties of the base material thereby retaining the excellent bulk properties [2].

Silicon carbide (SiC) has excellent mechanical properties such as extreme hardness and high wear resistance [3]. Accordingly, SiC is a choice material for coating the surface of engineering materials in order to confer higher hardness and wear resistance on them. However, high temperature coating processes such as thermal spraying is not suitable for the deposition of SiC because it decomposes before melting [4]. An alternative to high temperature deposition of SiC that will prevent its thermal decomposition is the cold gas dynamic spraying (CGDS) process. The CGDS is a low temperature deposition process that uses a carrier gas to accelerates fine metal or alloy powders (1–50 μm in diameter) to supersonic velocities (300–1200 m s^{-1}) causing impact on a substrate and producing a dense, adherent coating [5]. The operating temperatures in the CGDS process are lower than the melting point of either the substrate or the sprayed materials. Hence, there is limited or no-melting during coating deposition. In CGDS, coating depends solely on severe plastic deformation of the spray particles, and is formed by material interlocking and mechanical bonding between the corresponding atoms of the substrate and the coating powder [6]. The CGDS is used for the improvement of surface-dependent properties, environmental and protective coatings of engineering components, and for producing thick deposits which is suitable for the repair and dimensional restoration of damaged or out-of-specification parts [7].

The supersonic velocities of the CGDS are attained by the use of a converging/diverging de Laval nozzle. Two systems of such nozzle are available, viz: the high pressure cold spray (HPCS) ($P > 1$ MPa), and low pressure cold spray (LPCS) systems ($P = 0.3$ to 1.0 MP) [8, 9]. Since coating formation in CGDS solely relies on plastic deformation of the powders, only metal powders are suitable feedstock for the process. Ceramics powders produce no coating but erosion of the surface [10]. Lioma et al., [11] reported that the deposition of the carbide particles is limited because of the hard and brittle nature which makes them to shatter and erode the substrate upon impact instead of deformation. The solution is to bind the carbide phase with a more ductile material. Thus, adhesion between the hard and brittle ceramic phase and the substrate can be achieved [12–14]. The successful deposition of carbide powders, and the properties of cold spray coatings (such as microhardness, porosity etc) depend on a lot of parameters such as gas temperature and pressure, standoff distance (SOD), substrate properties, powder particle size and morphology, and binder content. Of these parameters, the influence of gas temperature is more significant [15]. This is because the supersonic driving gas flow and the consequent particle acceleration behaviour are

* Corresponding authors.
E-mail addresses: adebiyidi@gmail.com (D.I. Adebiyi), PopoolaAPI@tut.ac.za (A.P.I. Popoola).

http://dx.doi.org/10.1016/j.matlet.2016.03.142
0167-577X/

significantly influenced by the temperature of the carrier gas. The deposition efficiency significantly improves as the carrier gas temperature increases [16].

Cold spray coating of relatively softer and ductile material such as Al with SiC based powder using the HPCS system has been studied [17, 18]. However, based on the current authors' knowledge, the deposition of SiC-based cermet on Ti-6Al-4V using the LPCS has not been reported in the literature. The current study therefore aims to investigate the feasibility of using Centerline SST low pressure CGDS system (Series P), with air as the carrier gas, to deposit a SiC-based cermet on Ti-6Al-4V. The effect of temperature of the carrier gas on the coating microstructure, porosity and hardness is discussed.

2. Experimental procedure

The feedstock powder for this investigation is a mechanical blend of 90 wt% SiC +5 wt%Al +5 wt% Ti. The substrate is Ti-6Al-4V ($35 \times 35 \times 5\ mm^3$) of nominal composition: 6.10 wt% Al, 4.01 wt% V, 0.15 wt% Fe, 0.007 wt% C, 0.12 wt% O, 0.005 wt% N, Ti, balance. Prior to the coating process, the substrates were grit blasted with $-300+100\ \mu m$ alumina grit (Centerline SST-G0002). This is necessary to facilitate adhesion of the feedstock powder to the substrate. The parameters for the coating deposition were: $V=3\ ms^{-1}$, feed rate setting =30%, $P=0.99$ Mpa, T=450, 500, 550 °C. These parameters were selected based on preliminary investigations [19]. Moreover, since the deposition of ceramics such the SiC usually requires the higher pressure, the maximum allowable pressure of the LPCS system (0.99 Mpa) was used. The samples were prepared for microstructural analysis following standard metallographic procedure [20]. The microstructure of the coatings were studied using SEM (JEOL JSM 7600 F FESEM), the phase constituents were characterized using XRD (Philips P1710 Panalytical) with Cu target K_α radiation. The samples were scanned at interval of 2θ and a step size of 0.02. The phases present were identified using X'Pert High score plus software. The percentage porosity of the coatings were analyzed using ImageJ software.

The hardness of the coatings were measured using Vickers hardness tester (Future Tech FM-ARS900) according to ASTM E384 [21] standard to ensure consistent result. A load of 100 g was allowed to dwell for 15 s [22, 23]. A total of ten indentations were made on each coating sample and the average is reported as the surface hardness of the sample.

3. Results and discussion

3.1. Microstructure and phase analysis

The SEMs of the initial powders are shown in Fig. 1. Fig. 1 (D) is a mechanical blend of the powders shown in Fig. 1 (A–C). As shown in Fig. 1 (D) homogenous distribution of the three powders was achieved in the feedstock powder.

The SEM of the cross-section of the coatings are shown in Fig. 2. No crack is observed in any of the coatings. The microstructure of the coating obtained at 500 °C has fewer pores as compared to other.

Fig. 3 shows the XRD of the coatings in comparison with that of the feedstock powder.

The SEMs of the coatings seem to consist mostly of the fine

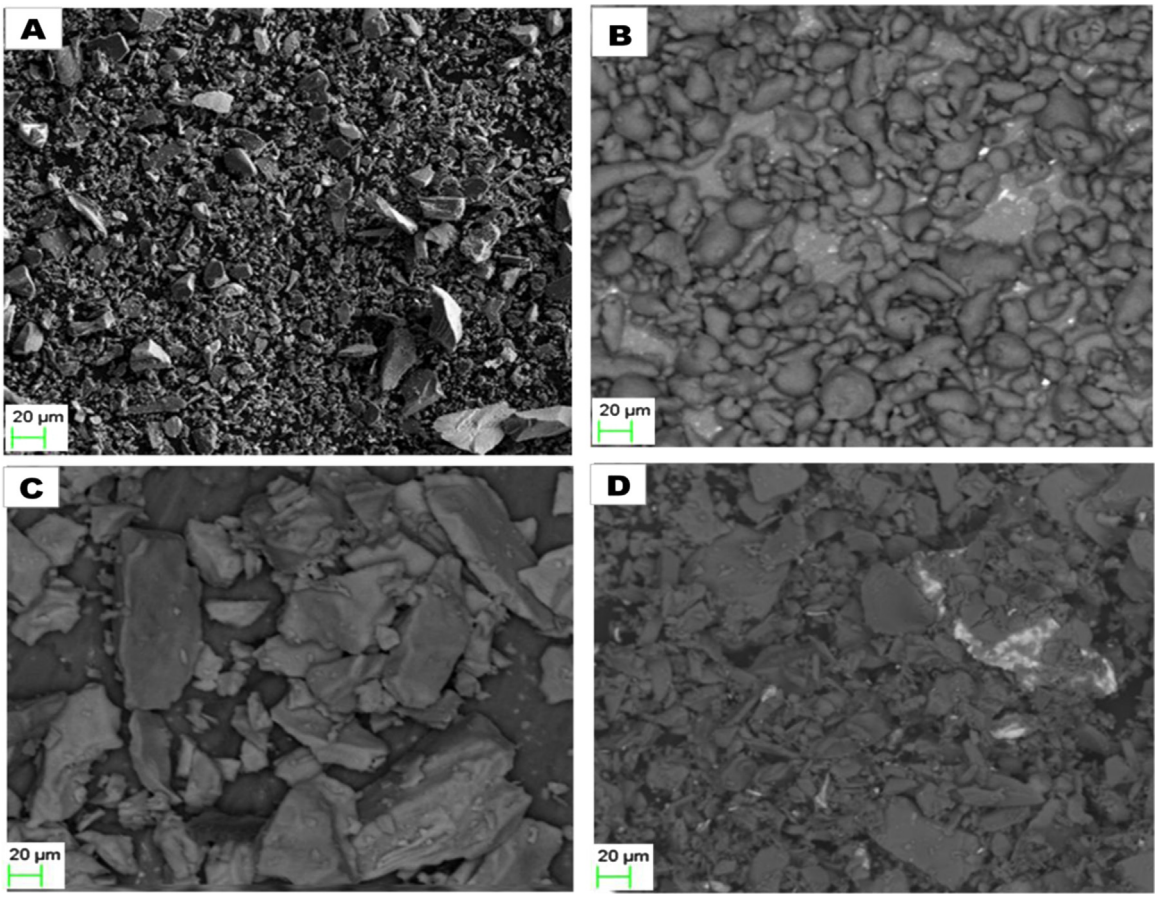

Fig. 1. Scanning electron micrographs of the feed stock powders: (A) SiC, (B) Al, (C) Ti, (D) SiC-5 wt% Al-5 wt% Ti.

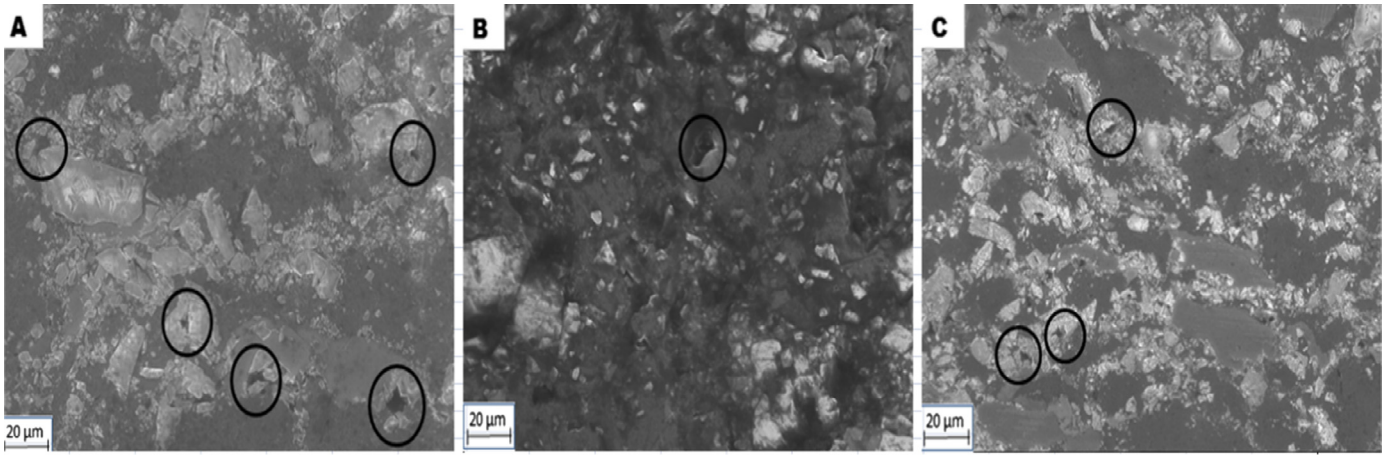

Fig. 2. Scanning electron micrograph of the Coatings: (A) 450 °C, (B) 500 °C, (C) 550 °C.

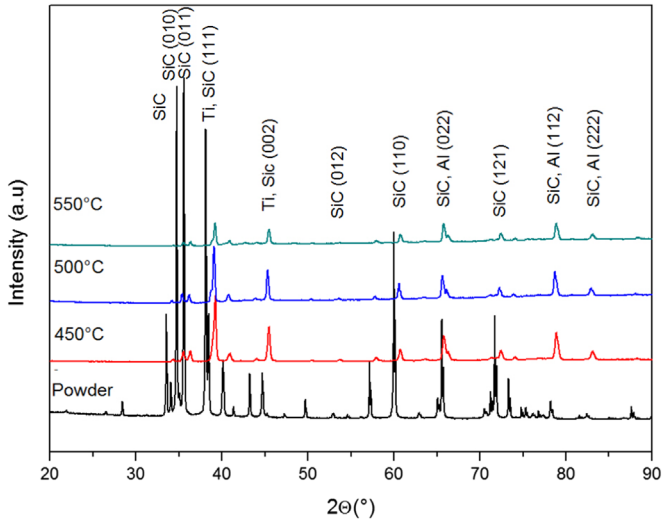

Fig. 3. XRD of the coatings in comparison with the feedstock powder.

particles in the feedstock powder. This could be attributed to higher deposition efficiency of smaller particles. Fine particles have higher deposition efficiency because particle acceleration varies inversely with the particle size. Hence, fine particles will attain critical velocity and have higher impact velocities than larger particles. Thus the fine particles would have impacted the substrate at higher velocities than the larger particles, making the fine particles able to deform the substrate and lodge in the coatings. On the contrary, the larger particles would not produce craters that are large enough to form coating and will therefore cause erosion rather than coating. However, there is no quantitative measurement of particle velocity in order to evaluate the relationship between the critical particle velocity and particle size. Further work is required to verify this. The XRD in Fig. 3 indicates that the diffraction pattern of the feed stock powder and the coatings are identical. This confirms that the cold spray coating carried out in this work did not lead to phase transformation, decomposition and/or decarburization as opposed to what is usually observed during thermal spray of SiC. However, a peak shift is observed between the phases in the feedstock powder and the coatings. This could be as a result of change (decrease) in lattice parameters caused by the micro-straining, amophization and grain refinement which would have occurred by virtue of the high impact of blending and high-velocity deposition process. Moreover, there is possible formation of impact-induced vacancies and carbon antisite in the SiC structure, which can lead to the formation of a SiC-C solid solution [24].

Moreover, the SiC particles in the feedstock powder were not deformed; their features in the feedstock powder remained unchanged in the coating. This is probably because the pressure and velocity of the LPCS system were not sufficient to deform the SiC. The deformation of SiC at the experimental temperature (450–550 °C) requires approximately 570 MPa [25]. It should have been expected that Al particles will experience greater deformation at 550 °C because particles have higher impact velocities at higher gas temperature which leads to greater deformation. However, as seen in the SEM, Al particles have highest deformation at 500 °C. This is probably because thermal softening would have taken place at 550 °C since Al melts at 660 °C.

The precipitation of Ti-Al intermetallics (TiAls) such as TiAl, $TiAl_3$, $TiAl_5$ etc has been reported during high temperature processing of Ti-6Al-4V [1]. In addition, the presence of Al and Ti in the feedstock powders is expected to favour the formation of TiAls [26, 27]. However, the formation of TiAls was not observed in the coatings. This could be due to the limited solubility of titanium and aluminium in each other which necessitates a longer contact time between Al and Ti before TiAl could be formed [26]. The supersonic speed of the cold spray process does not favour this, it only allows a little contact time between Ti and Al. Moreover, the precipitation of TiAls requires higher temperature and pressure [26] than those used in this work.

3.2. Porosity

The coatings generally have fully dense structures, uneven surfaces, and minimal unconnected pores and partial homogenous distribution of SiC. Their porosity ranged between 3.22 and 3.95 as shown in Table 1. The coating-substrate interface shows no visible evidence of cracking or delamination, but roughness. Cracking of SiC and other ceramic particles during cold spray coating that was reported by previous authors [17, 18, 28] was not observed in the coatings. This is probably because the particle size of the SiC in this

Table 1
Properties of the coating.

Gas temperature (°C)	Hardness ($HV_{0.3}$)	Porosity (%)	Yield strength (GPa)	Tensile strength (GPa)
–	291 ± 13.9	–	0.92	0.69
450	599 ± 14.8	3.95	1.95	1.41
500	652 ± 12.7	3.22	2.45	1.78
550	634 ± 13.5	3.87	2.07	1.50

work is finer (−53 μm). This also explains why the porosity is minimal because SiC is hard and brittle, and larger SiC particle usually fractures to form pores at the Al-SiC boundary [18].

Porosity is sometimes a microstructural defect in cold spray coating; it determines the quality of coating and can significantly affect the coating properties and performance both positively and negatively depending on application [29, 30]. High porosity benefits a thermal barrier coating because it results in a low thermal conductivity. However, high level of porosity reduces mechanical properties [31]. A low porosity level is required for increasing hardness values [32]. According to Gnaeupel-Herold et al. [33], hardness increases as porosity decreases. Dong [31] reported that the porosity of thermal sprayed coatings ranges from several percent to 20%, Fauchais and Vardelle, [34] reported 3–8% for plasma sprayed coatings, and Lioma, et al. [13] obtained between 3.51% and 5.11% for WC-12 Co coating which resulted in higher hardness of the substrate.

Usually, higher gas temperature benefits impact velocity and particle temperature [35], leading to increase in the velocity of in-flight particles and decrease in volume fraction of porosity in the coatings. Contrarily, the highest temperature (550 °C) did not yield the lowest porosity. This is probably because, at 550 °C, Al particles would have experienced thermal softening, and this causes a decrease in critical velocity [36], reduced consolidation and increase in porosity.

3.3. Hardness

A general improvement in the surface hardness of the coating is observed for all the temperatures investigated as shown in Table 1. This hardness increase can be attributed to the following:

- The presence of the hard SiC ceramic particles in the feedstock powder. SiC has a Vickers hardness of 2350 [37].
- Strain hardening caused by the plastic deformation of the particle during cold spray deposition.
- Accumulated strain as a result of particle deformation due to the high impact of blending and supersonic deposition processes.

Among the coatings, the sample deposited at 500 °C has the highest average hardness of 652 ± 12.7 $HV_{0.3}$ which is more than twice the 291 ± 13.9 $HV_{0.3}$ obtained in the as-received (AR). The coatings deposited at 450 and 550 °C $HV_{0.3}$ have 599 ± 14.8 $HV_{0.3}$ and 634 ± 13.5 $HV_{0.3}$ respectively.

The coating deposited at 550 °C should have been expected to have the highest hardness because increase in gas temperature causes increase in: average kinetic energy of the molecules of the gas, particles temperature and impact velocity. This will increase the momentum of the powder particles, producing greater particle impact, higher work hardening effect, greater coating densification and increased coating microhardness. On the contrary, the highest hardness was obtained in the coating deposited at temperature of 500 °C. The coating deposited at 550 °C did not yield the highest hardness probably because of the thermal softening effect explained in Section 3.2 which may prevent plastic deformation, and lessen both strain hardening and hardness.

Although an increase in hardness is obtained in all the coatings, the hardness values are still less than those fabricated by high pressure cold spraying and high temperature process such as laser alloying. The comparatively lower hardness obtained in this work is probably because SiC did not decompose. SiC decomposes at temperature 2830 °C [38] producing mainly Si, Si_2C and SiC_2 according to the following equation [39]:

$$4SiC(s) = Si\ (g) + Si_2C\ (g) + SiC_2\ (g) + C(s)$$

The Si, Si_2, SiC_2 phases are much harder. Moreover, decomposition also causes the release of gaseous carbon which diffuses into the matrix, causing hardness increase.

According to Cahoon et al., [40], tensile and yield strengths can be determined from (Eqs. (1) and 2) [41]. The calculated values form these equations are included in Table 1.

$$TS = \left(\frac{H}{2.9}\right)\left(\frac{n}{0.217}\right)^n \quad (1)$$

$$YS = \left(\frac{H}{3}\right)(0.1)^n \quad (2)$$

H is the vicker's hardness number, and n is the strain hardening coefficient, taken to be 0.15 [1]. The results show that both the yield and tensile strengths for the coatings have improved as compared to the substrate.

4. Global analysis

The gas temperature of 450 °C yielded a porosity level of 3.95% and a hardness value of 599 ± 14.8. The porosity was 3.87% and the hardness value was 634 ± 13.5 when the gas temperature was increased to 550 °C. Optimum gas temperature of 500 °C yielded the lowest porosity of 3.22% and a corresponding highest hardness value of 652 ± 12.7. Accordingly, the highest temperature did not yield the best coating properties. However, the lower the porosity of the coating, the higher the hardness and the better the surface mechanical properties.

5. Conclusion

Cold spray coating of Ti-6Al-4V with SiC-based cermet using the low pressure CGDS is plausible. No phase transformations, decarburizations or decompositions were observed in the coatings but a peak shift between the feedstock powder and the coatings. This is traced to microstraining, amophization and grain refinement caused by the high impact of the blending and cold spray processes. The coatings are fully dense with minimal non-connected pores. The distribution of SiC within the coating was partially homogenous and led to improvement in coating hardness to a maximum of 652 ± 12.7$HV_{0.3}$ from 291 ± 13.9 in the substrate.

Acknowledgements

This material is based upon work supported financially by the National Research Foundation (NRF). The authors also acknowledge the support from the African Laser Centre and the Tshwane University of Technology, Pretoria, South Africa which helped to accomplish this work.

References

[1] D.I. Adebiyi, A.P.I. Popoola, Mitigation of abrasive wear damage of Ti–6Al–4V by laser surface alloying, Mater. Des. 74 (2015) 67–75.
[2] H. Sahasrabudhe, J. Soderlind, A. Bandyopadhyay, Laser processing of in situ TiN/Ti Composite Coating on Titanium, J. mech. Behav. Biomed. Mat. 53 (2016) 239–249.
[3] Ravindra D, Patten J, (2009). Ductile regime single point diamond turning of CVD-SiC resulting in an improved and damage-free surface. In 4th International Conference on Recent Advances in Materials, Minerals & Environment and 2nd Asian Symposium on Materials & Processing, Penang, Malaysia.
[4] M. Tului, B. Giambi, S. Lionetti, G. Pulci, F. Sarasini, T. Valente, Silicon carbide based plasma sprayed coatings, Surf. Coat. Technol. 207 (2012) 182–189.
[5] A. Papyrin, V. Kosarev, S. Klinkov, A. Alkhimov, V.M. Fomin, Cold Spray

Technol, Elsevier, 2006.
[6] N.M. Melendez, V.V. Narulkar, G.A. Fisher, A. McDonald, Effect of reinforcing particles on the wear rate of low-pressure cold-sprayed WC-based MMC coatings, Wear 306 (2013) 185–195.
[7] V.K. Champagne, D.J. Helfritch, Mainstreaming cold spray–push for applications, Surf. Eng. 30 (6) (2014) 396–403.
[8] M. Gardon, A. Latorre, M. Torrell, S. Dosta, J. Fernandez, J.M. Guilemany, Cold spray titanium coatings onto biocompatible polymer, Mater. Lett. 106 (2013) 97–99.
[9] K.H. Ko, J.O. Choi, H. Lee, Y.K. Seo, S.P. Jung, S.S. Yu, Cold spray induced amorphization at the interface between Fe coatings and Al substrate, Mater. Lett. 149 (2015) 40–42.
[10] A. Sova, V.F. Kosarev, A. Papyrin, I. Smurov, Effect of ceramic particle velocity on cold spray deposition of metal-ceramic coatings, J. Therm. Spray. Technol. 20 (2011) 285–291.
[11] D. Lioma, N. Sacks, I. Botef, Cold gas dynamic spraying of WC–Ni cemented carbide coatings, Int. J. Refractory Met. Hard. Mater. 49 (2015) 365–373.
[12] J. Wang, J. Villafuerte, Low pressure cold spraying of tungsten carbide composite coatings, Advan. Mater. Process. 167 (2009) 54–56.
[13] N.M. Melendez, A.G. McDonald, Development of WC-based metal matrix composite coatings using low-pressure cold gas dynamic spraying, Surf. Coat. Technol. 214 (2013) 101–109.
[14] E. Sansoucy, P. Marcoux, L. Ajdelsztajn, B. Jodoin, Properties of SiC-reinforced aluminum Alloy Coatings produced by the Cold Gas Dynamic spraying process, Surf. Coat. Technol. 202 (2008) 3988–3996.
[15] P. Cavaliere, A. Silvello, Processing parameters affecting cold spay coatings performances, Inter. I J. Adv. Man. Tech. 71 (1–4) (2014) 263–277.
[16] S. Yin, X. Suo, H. Liao, Z. Guo, X. Wang, Significant influence of carrier gas temperature during the cold spray process, Surf. Eng. 30 (6) (2014) 443–450.
[17] Y. Wang, B. Normand, N. Mary, M. Yu, H. Liao, Microstructure and corrosion behavior of cold sprayed SiC p/Al 5056 composite coatings, Surf. Coat. Technol. 251 (2014) 264–275.
[18] M. Yu, X.K. Suo, W.Y. Li, Y.Y. Wang, H.L. Liao, Microstructure, mechanical property and wear performance of cold sprayed Al5056/SiCp composite coatings: effect of reinforcement content, App. Surf. Sci. 289 (2014) 188-96.
[19] Adebiyi D I, Botef I, Popoola P A. Computational technique for optimization of the process parameter for cold spray coating of titanium. In: 1st International Conference on Mathematical Methods & Computational Techniques in Science & Engineering, Athens, Greece; 2014, 239-243.
[20] Geels K, Fowler DB, Kopp WU, Ruckert M. West Conshohocken, PA: ASTM International, 2007.
[21] A.S.T.M. Standard, E384 (2010e2): Standard test method for Knoop and Vickers hardness of materials, ASTM Standards, ASTM International, West Conshohocken, PA, 2010.
[22] EPD Congress 2012, in: L. Zhang, J.A. Pomykala, A. Ciftja (Eds.), John Wiley & Sons, 2012, p. 34.
[23] S.S. Hosmani, P. Kuppusami, R.K. Goyal, An Introduction to Surface Alloying of Metals, Springer, 2014.
[24] M. Gadzira, G. Gnesin, O. Mykhaylyk, O. Andreyev, Synthesis and Structural peculiarities of nonstoichiometric β-SiC, Dia. Relat. Mater. 7 (1998) 1466–1470.
[25] A. Mussi, J. Rabier, L. Thilly, J.L. Demenet, Plasticity and deformation microstructure of 4 h-SiC below the brittle-to-ductile transition, Phys. Stat. Solid 4 (2007) 2929–2933.
[26] C. Xue, J.K. Yu, Z.Q. Zhang, In situ joining of titanium to SiC/Al composites by low pressure infiltration, Mater. Des. 47 (2013) 267–273.
[27] R. Jiangwei, L. Yajiang, F. Tao, Microstructure characteristics in the interface zone of Ti/Al diffusion bonding, Mater. Lett. 56 (2002) 647–652.
[28] W.Y. Li, G. Zhang, H.L. Liao, C. Coddet, Characterizations of cold sprayed TiN Particle reinforced Al2319 Composite Coating, J. Mater. Process. Technol. 202 (2008) 508–513.
[29] J. Villafuerte, Modern Cold Spray (2015).
[30] V.K. Champagne, The Cold Spray Materials Deposition process: Fundamentals and Applications, Elsevier, 2007.
[31] Surface engineering of light alloys: aluminium, in: H. Dong (Ed.), Magnesium and Titanium Alloys, Elsevier, 2010.
[32] D. Thirumalaikumarasamy, K.S. Kamalamoorthy, V.B. Visvalingam, Effect of experimental parameters on the micro hardness of plasma sprayed alumina coatings on AZ31B magnesium alloy, J. Magnes. Alloys 3 (3) (2015) 237–246.
[33] T. Gnaeupel-Herold, H.J. Prask, J. Barker, F.S. Biancaniello, R.D. Jiggetts, J. Matejicek, Microstructure, mechanical properties, and adhesion in IN625 air plasma sprayed coatings, Mat. Sci. Eng.: A 421 (1) (2006) 77–85.
[34] P. Fauchais, A. Vardelle, Thermal sprayed coatings used against corrosion and corrosive wear, INTECH Open Access Publisher, 2012.
[35] Huang RZ, Fukanuma H. The influence of Spray Conditions on Deposition Characteristics of Aluminum Coatings in Cold Spraying. Marple, BR; Hyland, 2009; MM; Lau, Y.-C: 279-84.
[36] C.J. Li, W.Y. Li, H. Liao, Examination of the Critical Velocity of Deposition of Particles in Cold Spraying, J. Therm. Spray. Techno 15 (2006) 212–222.
[37] L.A. Medica, Guidelines for Safe handling of powders and Bulk Solids, Wiley, 2004.
[38] S. Mahajan, L.C. Kimerling, Concise Encyclopedia of semiconducting Materials & related Technologies, Elsevier, 2013.
[39] E.K. Sanchez, T. Kuhr, V.D. Heydemann, V.W. Snyder, G.S. Rohrer, M. Skowronski, Formation of thermal decomposition cavities in physical vapor transport of silicon carbide, J. Elect. Mater. 29 (2000) 347–352.
[40] J.R. Cahoon, W.H. Broughton, A.R. Kutzak, The determination of yield strength from hardness measurements, Met. Trans. 2 (1971) 1979–1983.
[41] K.S. Chenna, G.N. Kumar, K. Jha Abhay, P. Bhanu, On the prediction of strength from hardness for copper alloys, J. Mater. (2013).